MENTATION PAGE

Form Approved
OMB No. 0704-0188

REPORT DATE	3. REPORT TYPE AND DATES COVERED
	Reprint

4. TITLE AND SUBTITLE
Effect of Nonequilibrium Phonons on the Electron Relaxation and Transport

5. FUNDING NUMBERS

6. AUTHOR(S)
M. Lax and W. Cai

7. PERFORMING ORGANIZATION NAME(S) AND ADDRESS(ES)
City College of the City University
of New York
NYC 10031

8. PERFORMING ORGANIZATION REPORT NUMBER

9. SPONSORING/MONITORING AGENCY NAME(S) AND ADDRESS(ES)
U. S. Army Research Office
P. O. Box 12211
Research Triangle Park, NC 27709-2211

10. SPONSORING/MONITORING AGENCY REPORT NUMBER

11. SUPPLEMENTARY NOTES
The view, opinions and/or findings contained in this report are those of the author(s) and should not be construed as an official Department of the Army position, policy, or decision, unless so designated by other documentation.

12a. DISTRIBUTION/AVAILABILITY STATEMENT
Approved for public release; distribution unlimited.

12b. DISTRIBUTION CODE

13. ABSTRACT *(Maximum 200 words)*

We review the recent theoretical study of the effect of nonequilibri um phonons on hot-carrier relaxation and transport. In a quantum well, the proper treatment of the electron-phonon coupling between electrons confined to two dimensions (2-D) by phonons traveling freely in three dimensions (3-D) requiares special care because phonon heating produces a bottleneck in the rate of transfer of energy from the carriers to the phonons. Because the carriers interact with phonons primarily when the latter are close to the quantum well, the latter should be described, not by plane waves, but by packets adapted to the shape of the carrier confinement. A quasi-equilibrium technique that retains off-diagonal elements in the phonon wave-vector permits an unrestrictedtreatment of the den-sityoperator equation. That in turn leads to a choice of wave packe that comes from solving the integrodifferential equations rather tha by imposition. Moreover, if the carrier distribution is assumed in quasi-equilibrium with a given drift and temperaure, the coupled

14. SUBJECT TERMS		15. NUMBER OF PAGES
nonequilibrium phonons	hot-carrier electron-phonon packets	16. PRICE CODE

17. SECURITY CLASSIFICATION OF REPORT	18. SECURITY CLASSIFICATION OF THIS PAGE	19. SECURITY CLASSIFICATION OF ABSTRACT	20. LIMITATION OF ABSTRACT
UNCLASSIFIED	UNCLASSIFIED	UNCLASSIFIED	UL

International Journal of Modern Physics B, Vol. 6, No. 7 (1992) 975–1006

EFFECT OF NONEQUILIBRIUM PHONONS ON THE ELECTRON RELAXATION AND TRANSPORT

M. Lax

Department of Physics, City College of New York, New York, N.Y. 10031 and AT&T Bell Laboratories, Murray Hill, New Jersey 07974.

W. Cai,

Department of Physics, City College of New York, New York, New York 10031

We review the recent theoretical study of the effect of nonequilibrium phonons on hot-carrier relaxation and transport. In a quantum well, the proper treatment of the electron-phonon coupling between electrons confined to two dimensions (2-D) by phonons traveling freely in three dimensions (3-D) requires special care because phonon heating produces a bottleneck in the rate of transfer of energy from the carriers to the phonons. Because the carriers interact with phonons primarily when the latter are close to the quantum well, the latter should be described, not by plane waves, but by packets adapted to the shape of the carrier confinement. A quasi-equilibrium technique that retains off-diagonal elements in the phonon wave-vector permits an unrestricted treatment of the density operator equation. That in turn leads to a choice of wave packet that comes from solving the integrodifferential equations rather than by imposition. Moreover, if the carrier distribution is assumed in quasi-equilibrium with a given drift and temperature, the coupled partial differential equations are reduced to coupled ordinary differential equations that can be solved with modest computer power. Comparison with experimental results for steady flow of energy from carriers to phonons, and for time-dependent relaxation yields quantitative agreement.

1. THE PROBLEM

The production of microelectronic devices by molecular beam epitaxy, and the high mobility of carriers particularly in modulated heterostructures created the importance of this area of study. Moreover, for transport in small high mobility systems, moderate voltages can lead to strong fields and non-linear effects. An excellent review of two-dimensional transport, with an extensive list of references has been given by Ando, Fowler, and Stern[1]

There already was experimental evidence by Shah *et al*[2,3] and Ryan *et al*[4] that the rate of energy transfer from electrons to phonons was an order of magnitude less than perturbation theory would yield.[5-7] On the other hand, controversial experimental results were also reported by Yang *et al*.[8] Several causes that may contribute to this reduction of the energy-loss rate were considered. The first one is the effect of reduced dimensionality. Theory[5-7] showed merely insignificant dependence of the energy-loss rate on dimensionality, when the predominant loss is by emission of longitudinal-optical (LO) phonons. The second is screening of electron-phonon interaction by free carriers. Screening has been appraised by Rühle *et al*[9] to play only a minor role up to electron densities of $n = 10^{17}$ cm^{-3}.

It was clearly perceived by the experimentalists, and a qualitative theory was developed by Price,[10] that the inability of the longitudinal optical (LO) phonon system to dissipate heat fast enough was creating a bottleneck. A reabsorption of phonon energy by electrons is presumed to decelerate carrier cooling. In fact, this bottleneck effect has been discussed by Pötz and Kocevar[11] in the 3D case. In the 2-D case, Price's theory is qualitative, because he was forced to introduce an ad hoc parameter - the number of phonons that interact with an electron: Price recognized the need, and called for a more rigorous treatment.

2. OUR RESOLUTION

During that time, I (M. Lax) perceived a need for understanding electron (and hole) transport in quantum wells and heterostructures and hired two research associates, W. Cai and M. C. Marchetti, to work in this area. Cai was already an expert in semiconductor physics and Marchetti an expert on transport in liquids. My role was advice and criticism.

We concluded[12,13] that the problem was a general one: how should electrons, whose transport is confined to two dimensions, interact with phonons that can propagate freely in three dimensions. More specifically, since the electrons only interact with phonons when they are in the vicinity of the quantum well, a plane wave description for the phonons is inconvenient. One possibility is to retain the plane wave description, but quantize the phonons (in the z direction) over a thickness L comparable to the well width. But such a treatment would be equivalent to Price's with L as the arbitrary parameter.

Cai proposed a resolution of this problem by using a basis set for the z direction (normal to the well walls) that consists in a Gaussian times a set of Hermite polynomials. But it was not known how many terms were needed. The use of a single term, the Gaussian, has as an arbitrary parameter, the width of the Gaussian.

2.1. Quasi-Equilibrium

After reviewing the work, I suggested that the shape of the phonon "packet" should come out of the problem, not be imposed. Marchetti then suggested the use of a quasi-equilibrium procedure of the sort introduced by Bogolyubov in dealing with classical liquid transport and by Zwanzig[14,15] in a variety of problems. See also Zubarev[16] and Peletminskii and Yatsenko[17] The basic idea is the quasi-equilibrium assumption that the variables of a problem can be divided into slow variables and fast ones. The fast variables are assumed to be in equilibrium with the current values of the slow variables. When the fast variables are inserted into the equations for the slow ones, we get an effective set of equations for the slow variables.

2.2. The Choice of Slow Variables

The success of such a procedure clearly depends on the appropriate choice of slow variables. The electronic variables $a^{\dagger}_{n\mathbf{k}}a_{n\mathbf{k}}$ describe the occupancy of a state of transverse momentum $\mathbf{k}$ in the nth subband. The average of this set of variables

$$f_{n\mathbf{k}}(t) = \langle a^{\dagger}_{n\mathbf{k}}a_{n\mathbf{k}} \rangle \tag{2.1}$$

is the familiar distribution function for these carriers. These variables must clearly be included in the slow set.

The phonons are described by the three-dimensional wave vector

$$\mathbf{Q} = (\mathbf{q}, q_z) \tag{2.2}$$

associated with a plane wave representation $\exp(i\mathbf{Q}\cdot\mathbf{R})$. The variables to be used in this case are $b^{\dagger}_{\mathbf{q},q_z}b_{\mathbf{q}q'_z}$ with average value.

$$n_{\mathbf{q}}(q_z, q'_z) = \langle b^{\dagger}_{\mathbf{q},q_z}b_{\mathbf{q}q'_z} \rangle \tag{2.3}$$

Marchetti made the crucial proposal to retain the off-diagonal elements in Eq. (2.3). Although the work starts in the plane-wave representation, by allowing off-diagonal elements with respect to q_z, we have prepared the way for an eventual transformation to packets whose shape is as yet unknown.

2.3. Description of the Hamiltonian

The Hamiltonian $\hat{H}$ consists in an electron part $\hat{H}_e$, a phonon part $\hat{H}_p$, an electron-phonon interaction $\hat{V}_{ep}$ and a phonon-phonon interaction $\hat{V}_{pp}$ with

$$\hat{H}_e = \sum_{n,\mathbf{k}} E_{n\mathbf{k}}\, \hat{a}^{\dagger}_{n\mathbf{k}}\, \hat{a}_{n\mathbf{k}} \tag{2.4}$$

where $E_{n\mathbf{k}}$ is the energy associated with the state

$$\Psi_{n,\mathbf{k}}(\mathbf{r}, z) = A^{-1/2}\zeta_n(z)\exp(i\mathbf{k}\cdot\mathbf{r}) , \tag{2.5}$$

associated with the transverse wave-vector $\mathbf{k}$, and quantum well state n. Here $\zeta_n(z)$ is the n−th quantum state in the well. The unperturbed phonon part is

$$\hat{H}_p = \sum_{\mathbf{Q}} \hbar\omega_L\, \hat{b}^{\dagger}_{\mathbf{Q}}\hat{b}_{\mathbf{Q}} \tag{2.6}$$

$\mathbf{Q} = (\mathbf{q}, q_z)$

The electron-phonon interaction is given by the Fröhlich interaction [18]

$$\hat{V}_{ep} = \int d\mathbf{R} \int d\mathbf{R}'\, e\, \hat{n}(\mathbf{R})\, \frac{1}{|\mathbf{R}-\mathbf{R}'|}[-\nabla'\cdot\hat{\mathbf{P}}(\mathbf{R}')] , \tag{2.7}$$

namely, the Coulomb interaction between the electron charge density $e\hat{n}$ and the charge density $-\nabla\cdot\mathbf{P}$, where $\mathbf{P}$ is the phonon induced polarization, so that

$$\hat{V}_{ep} = \frac{i\alpha}{\sqrt{A}} \sum_{n,\mathbf{k}} \sum_{n',\mathbf{k}'} \sum_{\mathbf{Q}} \left\{ \hat{b}_{\mathbf{Q}}\, \delta_{\mathbf{k}',\,\mathbf{k}+\mathbf{q}}\, G_{n'n}(\mathbf{q}, q_z) - \hat{b}^{\dagger}_{\mathbf{Q}}\, \delta_{\mathbf{k}',\,\mathbf{k}-\mathbf{q}}\, G^{*}_{n'n}(\mathbf{q}, q_z) \right\} \hat{a}^{\dagger}_{n'\mathbf{k}'}\hat{a}_{n\mathbf{k}} , \tag{2.8}$$

where the matrix element G takes the form

$$G_{n'n}(\mathbf{q}, q_z) = \frac{1}{Q\sqrt{L}} \int_{-\infty}^{+\infty} dz\, \zeta^{*}_{n'}(z)\, \exp(iq_z z)\, \zeta_n(z). \tag{2.9}$$

In Eq. (2.8), α is the Fröhlich interaction constant[18]

$$\alpha = [2\pi e^2\hbar\omega_L(1/\varepsilon_\infty - 1/\varepsilon_0)]^{1/2} . \tag{2.10}$$

2.4. Form of the Equations of Motion

One can derive the kinetic equations for a set of macroscopic observables, $\{\gamma_i(t)\}$ from the quantum-mechanical Liouville equation. Here we choose the following observables: $\{\gamma_i(t)\} = \{ f_{n\mathbf{k}}(t),\ n_{\mathbf{q}}(q_z, q_z', t)\}$ (see Eqs. (2.1) and (2.3)). If the Liouville equation is solved to the lowest order, the rate of change of any function of $\gamma(t)$, denoted by $F(\gamma(t))$, is given by

$$\frac{\partial F(\gamma(t))}{\partial t} = \frac{i}{\hbar}\mathrm{Tr}[\,\hat{H}_0(t),\, F(\hat{\gamma}(t))\,]\hat{\rho}_0(t) + \left|\frac{i}{\hbar}\right|^2 \lim_{\varepsilon\to 0^+} \int_{-\infty}^{0} d\tau\, e^{\varepsilon\tau}\, \mathrm{Tr}\{[\,\hat{V}(\tau),\,[\hat{V}, F(\hat{\gamma})]\,]\hat{\rho}_0(t)\} , \tag{2.11}$$

where $\hat{V}(\tau)$ is the coupling perturbation in the interaction representation:

$$\hat{V}(\tau) = \exp[(i/\hbar)(\hat{H}_e + \hat{H}_P)\tau]\,\hat{V}\exp[(-i/\hbar)(\hat{H}_e + \hat{H}_P)\tau]\,\hat{V} \tag{2.12}$$

and $\hat{\rho}_0(t)$ the unperturbed density matrix. Here, neither the electron nor the phonon system is assumed to be even close to equilibrium. From Eq. (2.11), we obtain coupled integrodifferential equations of the form

$$\frac{\partial f_{n\mathbf{k}}}{\partial t} = \sum_{q}\sum_{q_z}\sum_{q_z'}\sum_{n'\mathbf{k}'} M[f_{n\mathbf{k}}, f_{n'\mathbf{k}'}, n_{\mathbf{q}}(q_z, q_z', t)] \tag{2.13}$$

$$\left[\frac{\partial n_{\mathbf{q}}(q_z, q_z', t)}{\partial t}\right]_{ep} = \sum_{n\mathbf{k}}\sum_{n'\mathbf{k}'}\sum_{q_z''} f_{n\mathbf{k}}[1 - f_{n'\mathbf{k}'}] \times [\text{Four terms}]. \tag{2.14}$$

where a typical term is given by

$$\delta_{\mathbf{k}',\,\mathbf{k}-\mathbf{q}}\,\frac{G_{n'n}(\mathbf{q}, q_z)\,G^*_{n'n}(\mathbf{q}, q_z'')}{\varepsilon - i[E_{n\mathbf{k}} - E_{n'\mathbf{k}'} - \hbar\omega_L]}[\delta_{q_z'', q_z'} + n_{\mathbf{q}}(q_z'', q_z', t)] \tag{2.15}$$

The detailed equations will be presented in the Appendix. Here we emphasize their form. In particular, let us regard $\mathbf{q}$ and q_z' as parameters. Then Eq. (2.14) with Eq. (2.15) has the form (for the term shown in Eq. (2.15))

$$\frac{\partial n(q_z, t)}{\partial t} = \Phi(q_z, t) + K(q_z)M(t) \tag{2.16}$$

where

$$M(t) = \int H(q_z'')n(q_z'', t)dq_z'' \tag{2.17}$$

after all parameters such as $\mathbf{q}, q_z'$ are suppressed. Multiplication of Eq. (2.15) by $H(q_z)$ and integration leads to the reduced *ordinary differential* equation

$$\frac{dM(t)}{dt} = I(t) + AM(t) \tag{2.18}$$

where

$$I(t) = \int H(q_z)\Phi(q_z, t)dq_z \quad ; \quad A = \int H(q_z)K(q_z)\,dq_z \tag{2.19}$$

2.5. The Shape of the Packet

Not only is the remaining computational task greatly simplified, Eq. (2.17) already informs us that (aside from a choice of normalization) the phonon wave-packet operators are

$$\hat{c}^{\dagger}_{n'n} \sim \sum_{q_z} G^*_{n'n}(\mathbf{q}, q_z)\hat{b}^{\dagger}_{\mathbf{q},q_z} \tag{2.20}$$

If there are S subbands of importance, there is one packet operator for each choice of (n', n) or $S(S+1)/2$ differently shaped packets. For the important case in which only the

$n = 0$ states participate there is one such packet (for each $\mathbf{q}$):

$$G_{00}^{*}(\mathbf{q}, q_z) = \frac{1}{N_L} \int_{-\infty}^{\infty} |\zeta_0(z')|^2 dz' \frac{\exp(-iq_z z')}{\sqrt{q^2 + q_z^2}} \tag{2.21}$$

The shape of this packet in ordinary share may be obtained by multiplication by $\exp(iq_z z)$ and integrating over q_z:

$$\frac{1}{N_L} \int R(z - z') dz' |\zeta_0(z')|^2 \tag{2.22}$$

where

$$R(z - z') = \int \frac{\exp[iq_z(z - z')]}{\sqrt{q^2 + q_z^2}} dq_z = 2K_0(q|z - z'|) \tag{2.23}$$

has the form of a modified Bessel function. This form arises from the Coulomb nature of the interaction. If we had used a point interaction $(q^2 + q_z^2)^{-1/2}$ would have been replaced by unity and $R(z - z')$ by $\delta(z - z')$ so that the packet shape would simply be $|\zeta_0(z)|^2$. More generally, the packet shape is a convolution of the electron density $|\zeta_0(z)|^2$ with $K_0(q|z - z'|)$ for each q.

2.6. Further Simplifications

We have not written the explicit form of the phonon-phonon interaction $\hat{V}_{pp}$ by means of which the relevant longitudinal optical phonons decay into acoustic phonons because we have replaced that process by a relaxation process of the form

$$\left[\frac{\partial n_{\mathbf{q}}(q_z, q_z', t)}{\partial t}\right]_{pp} = -\frac{n_{\mathbf{q}}(q_z, q_z', t) - \delta_{q_z, q_z'} n_L}{\tau_{op}}, \tag{2.24}$$

where the decay time for optical phonons τ_{op} has been estimated in the experimental papers[19] to be 7 psec.

For times larger than a picosecond it has been found by Monte Carlo calculations[20-23] and by our own quasi-analytical procedure[24] that the electron distribution has equilibrated relative to two macroscopic parameters: an electron temperature $T_e(t)$ and a drift velocity $\mathbf{v}_e(t)$, both of which may be time dependent. By introducing these parameters, the equation for the electron distribution is replaced by ordinary differential equations for these parameters.

Finally, since we have been dealing with variables such as $n_q(q_z, q_z')$ it was convenient to use a wave-packet construction on both left and right wave-vectors. Thus our reduced phonon variables are

$$N_{n'n,\,m'm}(q,\,t) = \frac{\sum\sum_{q_z q_z'} G^*_{n'n}(\mathbf{q},\,q_z)\, n_{\mathbf{q}}(q_z,\,q_z',\,t)\, G_{m'm}(\mathbf{q},\,q_z')}{F_{n'n,\,m'm}(q)/2q} \,, \tag{2.25}$$

where

$$F_{m'm,\,n'n}(q) = \int dz_1 \int dz_2\, \zeta^*_{n'}(z_1)\zeta_m(z_1)\zeta^*_n(z_2)\zeta_{n'}(z_2)\, e^{-q\,|z_1 - z_2|} \tag{2.26}$$

Thus, in general, we will get coupled ordinary differential equations for $T_e(t)$, $\mathbf{v}_e(t)$, and $N_{n'n,\,m'm}(t)$.

2.7. The reduced Equations

For simplicity, we shall write here only the special case in which only the lowest subband contributes. Thus we shall set

$$N_0(\mathbf{q},\,t) = N_{00,\,00}(\mathbf{q},\,t) \tag{2.27}$$

The phonon equation can then be written

$$\frac{\partial N_0(q,\,t)}{\partial t} = \frac{N_0(q,\,t)+1}{\tau_e(q,\,T_e(t))} - \frac{N_0(q,\,t)}{\tau_a(q,\,T_e(t))} - \frac{N_0(q,\,t) - N_L(T_L)}{\tau_{op}} \tag{2.28}$$

where the rate of phonon emission $1/\tau_e$ and the rate of phonon absorption $1/\tau_a$ are given by

$$\frac{1}{\tau_e(q,\,T_e)} = \frac{\pi\alpha^2}{\hbar}\,\frac{1}{q}\,\frac{F_{00,\,00}(q)\, I^{(+)}_{00}(q)}{|\,\varepsilon_{00,00}(q,\omega_L)\,|^2} \,, \tag{2.29}$$

$$\frac{1}{\tau_a(q,\,T_e)} = \exp\left[\,\hbar\omega_L/k_B T_e(t)\right]\,\frac{1}{\tau_e(q,\,T_e(t))} \,. \tag{2.30}$$

where $F_{00,\,00}(\mathbf{q})$ was defined in Eq. (2.26), and the matrix element $I^{(+)}$ is given by

$$I^{(+)}_{00}(q,\,T_e(t)) = \frac{m}{\pi^2\hbar^2 q}\int_{\frac{q}{2}+\frac{m\omega}{\hbar q}}^{\infty} kdk\,\frac{1}{|k^2 - (\frac{q}{2} + \frac{m\omega}{\hbar q})^2|^{1/2}}$$

$$\times f(E_k,\,T_e(t))\left[1 - f(E_k - \hbar\omega_L,\,T_e(t))\right] \,. \tag{2.31}$$

Eq. (2.30) shows that the ratio of rates of absorption and emission is governed by the instantaneous electron temperature. Dynamic screening effects are contained in the dielectric response function $\varepsilon_{00,00}(q,\,\omega_L)$ used in Eq. (2.29).

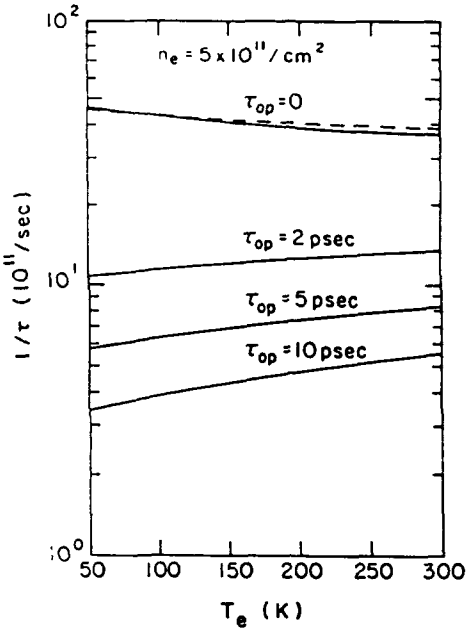

Fig. 1. $1/\tau$ as a function of the electron temperature T_e, for $\tau_{op}=0$, 2, 5, and 10 psec and $(n=0)$ lowest subband occupation. Dynamic screening is included (solid curves). The dashed curve shows for comparison a calculation for $\tau_{op}=0$ when static screening is used.[13] Comparison between the $\tau=0$ (no bottleneck case) and $\tau=10$ psec shows a reduction of one order of magnitude in the latter case.

2.8. Energy Loss Rate in Steady State Case

The first explicit calculation is made for the steady state case. In that case, the electron temperature $T_e(t) = T_e$ will be independent of time and assumed given. The problem is to calculate the rate of energy transfer from the electron gas into the LO phonons, and to express the result in the form used by the experimentalists. The latter fit their experimental data with an expression of the form:

$$P_e(t) = \frac{\hbar\omega_L}{\tau} \exp\left(-\frac{\hbar\omega_L}{k_B T_e}\right) \tag{2.32}$$

Then $1/\tau$ is plotted as a function of electron temperature.

We calculate $1/\tau$ by using the expression:

$$P_e(t) = \frac{\hbar\omega_L}{N_e}\sum_{\mathbf{q}}\frac{\partial n_{\mathbf{q}}(q_z, q_z, t)}{\partial t}\Big|_{ep}. \tag{2.33}$$

Comparison with the previous equation yields $1/\tau$. A plot of $1/\tau$ obtained in this manner is shown in Fig. 1.

We note that in the case in which $\tau_{op} = 0$, equilibration of the LO phonon modes takes place instantaneously. Thus no bottleneck effect will occur. But the effective energy transfer rate is reduced by an order of magnitude if one takes $\tau = 10$ psec. The dashed curve demonstrates that neglect of screening would have little effect on the results.

If we apply the steady state condition:

$$\frac{dN_0(\mathbf{q}, t)}{dt} = 0 \tag{2.34}$$

we can solve for $N_0(\mathbf{q})$, the non-equilibrium phonon occupancy associated with the transverse phonon wave-vector $\mathbf{q}$.

Using the Planck formula,

$$N_0(\mathbf{q}) = 1/\{\exp[\hbar\omega_L/k_B T(\mathbf{q})] - 1\} \tag{2.35}$$

the results can be expressed in the form of a temperature $T(\mathbf{q})$ for the phonons of a given transverse wave-vector $\mathbf{q}$. The results displayed in Fig. 2 show that the predominant heating occurs for small wave-vector phonons.

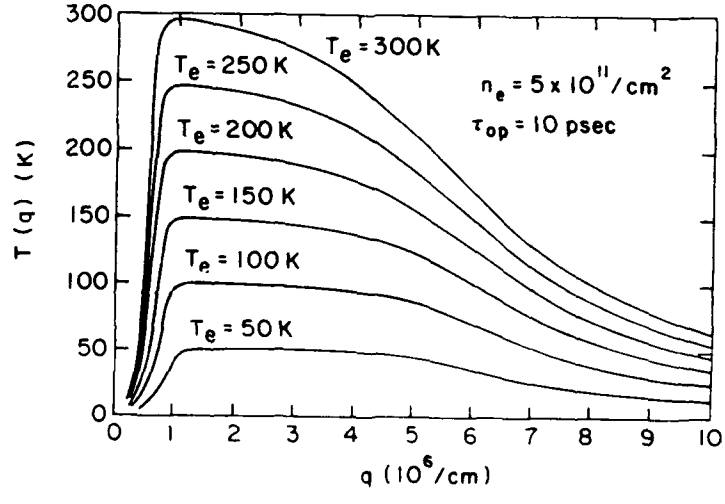

Fig.2 "Phonon temperature" $T(q)$ as a function of q for 50 K $\leq T_e \leq$ 300 K and lowest subband occupation.[13].

We have also made calculations when electrons and holes are simultaneously present,[25] and when more than one sub-band is occupied.[26] A comparison between experiment and theory for this case is shown in Fig. 3.

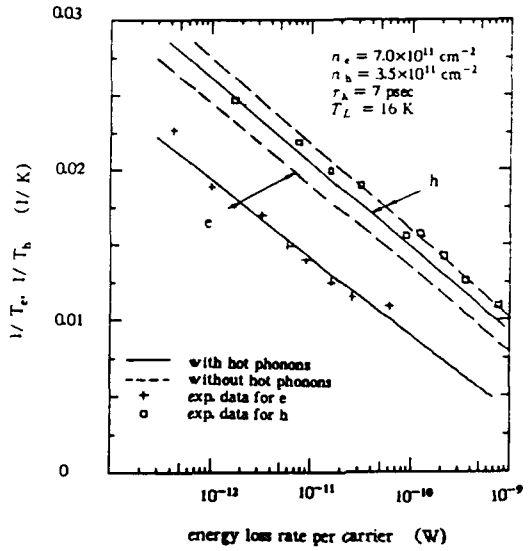

Fig. 3. The carrier temperature is plotted against the energy loss rate per carrier for the electron and hole case. For the electron case, the effect of hot phonons is found to be an order of magnitude, whereas for holes it is much less than an order of magnitude. The points are the experimental data of Shah et al.[27]

In Fig. 3 the curve for electrons is obtained by including only the polar interaction with LO phonons. The calculation for holes includes polar coupling to LO phonons and coupling to both LO and TO phonons via the deformation potential. Only heavy holes are considered. It is shown that the hot phonon effect is strong for electron relaxation, but is weak for hole relaxation. This follows because for holes the phonon emission rate $1/\tau_h(q)$ for given q, which is similar to Eq. (2.29) for $1/\tau_e(q)$, is much smaller than that for electrons. From Eqs. (2.29) and (2.31), we see that $1/\tau_e(q)$ is proportional to $f(E_k, T_e(t))$, which is proportional to $1/m$, with m the effective mass. The large effective mass of holes leads to a weaker build-up of hot phonons by the hole gas. On the other hand, heavy holes preferentially emit phonons with larger momentum $\mathbf{q}$, because of the large effective mass of hole. Therefore, the phase space of $\mathbf{q}$ that contributes to the total cooling rate for holes is much larger than that for electrons. This leads to the larger cooling rate for holes than that for electrons.

2.9. Time-dependent relaxation

Our starting equations are valid for the time-dependent case. We simply do not assume time derivatives vanish. The electron energy can be written as a sum over the transverse **k** vector:

$$<E_e(t)> = \frac{2}{A} \sum_{\mathbf{k}} E_{\mathbf{k}} f(E_{\mathbf{k}}, T_e(t)) \tag{2.36}$$

For simplicity, we again consider here only one sub-band. The rate of electron temperature change is then given by:

$$\frac{\partial T_e}{\partial t} = \frac{1}{C_v(T_e(t))} \frac{\partial <E(t)>}{\partial t} \tag{2.37}$$

where C_v is the specific heat: $C_v = \partial <E(t)> / \partial T_e(t)$. Since the phonon equations depend on the instantaneous temperature $T_e(t)$, we now have coupled ordinary differential equations connecting the phonon occupancies $N_0(\mathbf{q})$ and the electron temperature. It is assumed, of course, that $T_e(t = 0)$ is given. A comparison is given in Fig. 4 of our theoretical results with experiment [8].

As the electron gas relaxes, its temperature decreases as shown by the solid curve in Fig. 5. The associated rise in the phonon temperature is shown by the dashed curve which merges with the solid curve as the combined system relaxes to the lattice temperature. When τ_{op} is set equal to zero, the phonon bottleneck effect disappears, and the electron temperature falls more quickly as shown by the dot-dash curve.

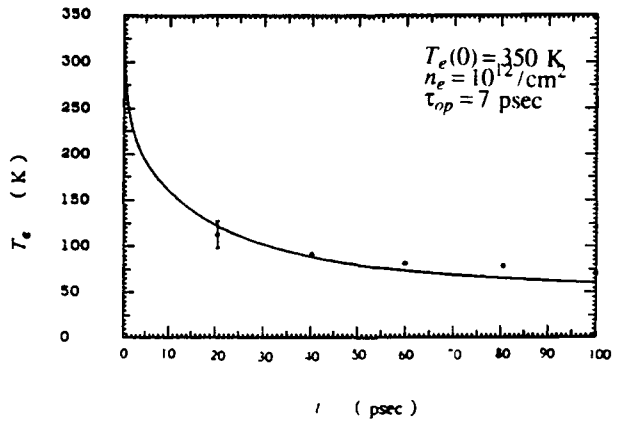

Fig. 4. Time dependent relaxation of an electron gas of density $n_e = 10^{12}$/cm^2 starting at an initial temperature of $T_e(0) = 350$K. The optical phonon decay rate has been given the accepted value of $\tau_{op} = 7$ psec. The experimental data are from Ryan *et al.*[4] corresponding to a 3D electron density $n = 5 \times 10^{18}/cm^3$ and to a maximum power absorbed by the sample of ~ 50 mW.

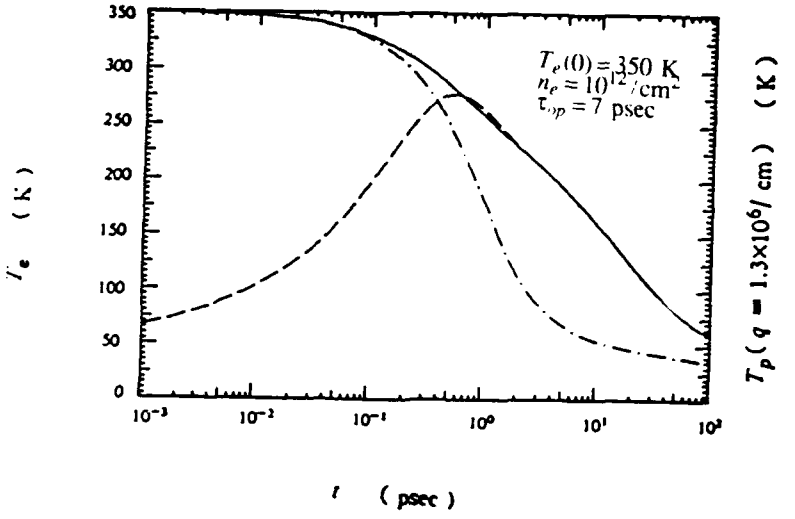

Fig. 5. A plot of electron temperature T_e against time (solid curve for $\tau_{op} = 7$ psec and dot-dash curve for $\tau_{op} = 0$) and of the phonon temperature $T_p(q)$ at $q = 1.3 \times 10^6 cm^{-1}$.

3. FURTHER APPLICATIONS OF THE THEORY

3.1. Hot electron transport

When a strong dc field is applied, the electron gas acquires an elevated temperature as well as a drift velocity. Moreover, the drift mobility is reduced more in the presence of a phonon bottleneck than in its absence. This issue was studied by Lei and Horing[28] and by us[29] The methods described earlier involving the introduction of a phonon packet remain valid. It is convenient, in addition to separate the center of mass motion of the electron gas from its relative motion. The density of electrons will again be assumed sufficiently high that the electron gas can be assumed in quasi-equilibrium with a given drift velocity and a given temperature. A term, which describes the center-of-mass motion under an applied field should be added upon to the Hamiltonian described in Sec. 2.3:

$$\hat{H}_c = \hat{\mathbf{P}}^2/2M - Ne\mathbf{E}\cdot\hat{\mathbf{R}}\ , \tag{3.1}$$

with $\hat{\mathbf{P}}$ and $\hat{\mathbf{R}}$ the center-of-mass momentum and coordinate operators, respectively, N the total number of electrons, and $M = Nm$, with m the electron effective mass. The electronic states are labeled by the 2D wave vector in the relative coordinate system, $\mathbf{k}$, and the discrete subband index, n; $\hat{a}^{\dagger}_{n\mathbf{k}}$ and $\hat{a}_{n\mathbf{k}}$ (Eq. (2.1)) now are the corresponding electron creation and annihilation operators in the relative coordinates and $E'_{n\mathbf{k}}$ is the energy of an electron in the

$(n, \mathbf{k})$ state. Therefore, the energy exchange of electron in the relative coordinates obeys the conservation condition:

$$E'_{n'\mathbf{k}'} - E'_{n\mathbf{k}} = \hbar(\omega_L - \mathbf{q}\cdot\mathbf{v}_e) , \tag{3.2}$$

with $\mathbf{v}_e$ the drift velocity of electrons. The intracollisional effect[30, 31], namely the effect of the electric field during the course of a collision can be neglected for the fields considered in our work[29]. If only the lowest subband is considered, we obtain a pair of time evolution equations for the drift velocity $\mathbf{v}_e$ and the total energy of electrons in the relative coordinates:

$$\frac{\partial M\mathbf{v}_e(t)}{\partial t} = -Ne\mathbf{E} - \sum_{\mathbf{q}} \hbar\mathbf{q} L_{e\text{-LO}}(\mathbf{q}, t) , \tag{3.3}$$

$$\left|\frac{\partial E'_e}{\partial t}\right|_{e\text{-LO}} = -\sum_{\mathbf{q}} (\hbar\omega_L - \mathbf{q}\cdot\mathbf{v}_e) L_{e\text{-LO}}(\mathbf{q}, t) . \tag{3.4}$$

Here

$$L_{e\text{-LO}}(\mathbf{q}, t) = \frac{2\pi\alpha^2}{\hbar}\left\{\sum_{q_z} G^*_{00}(\mathbf{q}, q_z) G_{00}(\mathbf{q}, q_z)\right\}$$

$$\times\{I^{(+)}_{00}(\mathbf{q}, \omega_{LO})[1 + N_0(\mathbf{q}, t)] - I^{(-)}_{00}(\mathbf{q}, \omega_{LO}) N_0(\mathbf{q}, t)\} , \tag{3.5}$$

where $N_0(\mathbf{q}, t)$ is defined by Eq. (2.27) and

$$I^{(\pm)}_{00}(\mathbf{q}, \omega_L) = \frac{2}{A}\sum_{\mathbf{k}}\sum_{\mathbf{k}'} f_{0\mathbf{k}}(t)\,[\,1 - f_{0'\mathbf{k}'}(t)]\,\delta_{\mathbf{k}',\mathbf{k}+\mathbf{q}}\,\delta(E'_{0\mathbf{k}} - E'_{0'\mathbf{k}'} \pm \hbar\mathbf{q}\cdot\mathbf{v}_e + \hbar\omega_L) , \tag{3.6}$$

where the electron distribution function in the relative coordinates $f_{0\mathbf{k}}(t)$ is assumed to be a Fermi-Dirac distribution with temperature $T_e(t)$. With the above approximations, the problem is again reduced to coupled ordinary nonlinear differential equations. Solving Eqs. (3.3) and (3.4) and corresponding equation for N_0, which is similar to Eq. (2.28), we can determine $\mathbf{v}_e$, T_e as well as $N_0(\mathbf{q})$

Results for the mobility reduction and temperature increase in a steady applied field are shown in Fig. 6.

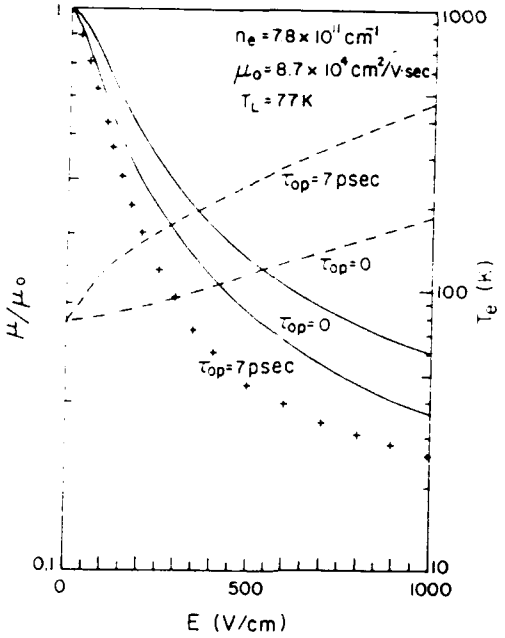

Fig. 6. The normalized mobility of electrons, $\mu(\mathbf{E})/\mu(\mathbf{E} \to \mathbf{0})$ (solid curves), and the electron temperature, T_e, (dashed curves) as functions of the external electric field $|\mathbf{E}|$ at $\tau_{op} = 0$ and $\tau_{op} = 7$ psec. The crosses represent the experimental data from Fig. 2(c) of Keever *et al*[32] at $T_L = 77$ K.

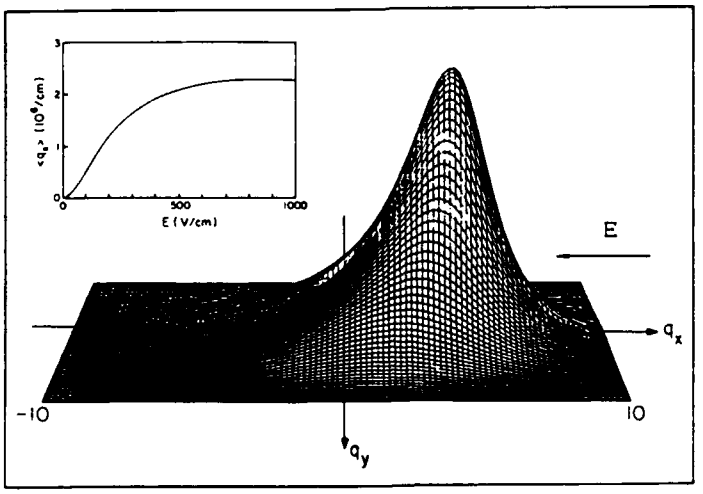

Fig. 7. "Optical phonon temperature", $T_{op}(\mathbf{q})$, as a function of $\mathbf{q}$ (unit: 10^6 cm^{-1}) at $|\mathbf{E}| = 500$ V/cm. The q_x-q_y plane represents $T_{op} = 77$ K, the peak value of T_{op} is 696 K. Inset: The average wave vector of nonequilibrium LO phonons, $< q_x >$, as a function of the electric field.

Phonon heating produced by the strong electric field is not isotropic, but is more effective for phonons whose propagation direction is in the direction of motion of the electrons. The phonons also acquire a mean "momentum" $<q_z>$. A contour plot of the phonon temperature rise, and an inset of the mean momentum are shown in Fig. 7.

We also studied the time evolution of electrons beginning from 'switch on' of a applied electric field until arrival at a steady state. Fig. 8 displays the results. The presence of hot phonons leads to time delay in arriving at a steady state.

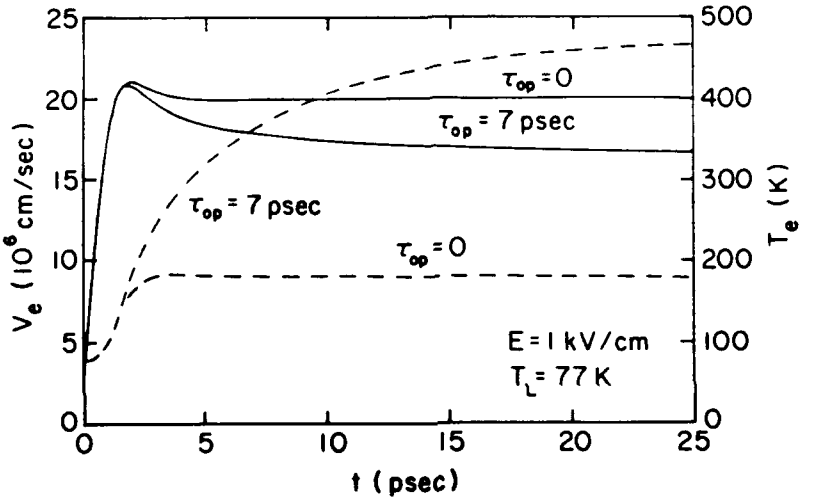

Fig. 8. The drift velocity of electrons, $|v_e|$ (solid curves) and the electron temperature, T_e (dashed curves) as functions of time t. The parameters are the same as those of Fig. 6.

3.2. Relaxation of the electron-hole plasma

When an undoped quantum well device is illuminated by a high-power laser, photo-excited electrons and holes are produced simultaneously. Therefore, it is necessary to study the cooling process of a photo-generated electron-hole plasma. This process involves, not only the carrier-phonon coupling, but also the electron-hole interaction. This issue was studied by Pötz[33] in bulk GaAs, and then by Marchetti and Pötz[34] in a GaAs-GaAlAs quantum well using the approach described above, since hot-phonon reabsorption can also slow down considerably the carrier cooling in the electron-hole plasma.

The energy of photo-excited electrons is assumed below that of the L valley, so intervalley scattering is not included. The carrier distributions are modeled as a time-dependent Fermi-Dirac distribution functions. The temperatures in the distribution functions for electrons and holes are allowed to be different to account for noninstantaneous energy transfer between two carrier systems. The equations for the time evolution of total electron energy (E_e) and

hole energy (E_h) is derived as

$$\frac{\partial E_e}{\partial t} = -R_{e-h} - R_{e-\mathrm{LO}} + R_L^e \,. \tag{3.7}$$

and

$$\frac{\partial E_h}{\partial t} = +R_{e-h} - R_{h-\mathrm{LO}} - R_{h-\mathrm{TO}} + R_L^h \,. \tag{3.8}$$

Here R_{e-h} is the power loss by electrons to holes via the screened Coulomb interaction. $R_{e-\mathrm{LO}}$ and $R_{h-\mathrm{LO}}$ are the rate of energy loss by carriers to LO phonons via the polar Fröhlich coupling, $R_{h-\mathrm{TO}}$ is the rate of energy loss by hole to TO phonons via the deformation potential coupling. R_L^e and R_L^h are the power input from the laser to electrons and holes, respectively. Only the lowest subband in the quantum well is considered.

The corresponding time evolution equations for non-equilibrium LO and TO phonons (similar to Eq. (2.28)) are coupled to Eqs. (3.7) and (3.8). Therefore, the temperatures T_e, T_h and the phonon distributions, $N_0^{\mathrm{LO}}(q)$ and $N_0^{\mathrm{TO}}(q)$, can be determined as function of time t.

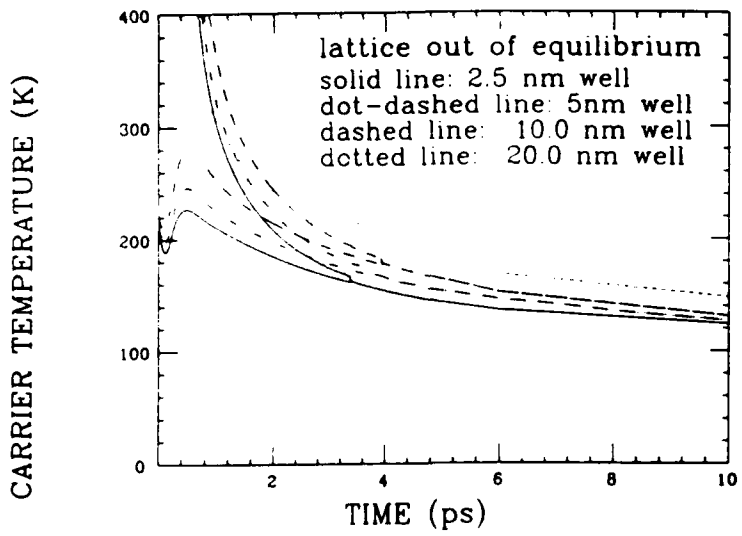

Fig. 9. Electron and hole temperatures as functions of time for $n_{2D} = 0.5\times10^{12}\,\mathrm{cm}^{-2}$ and four values of well thickness: $L = 25$ Å, solid line; $L = 50$ Å, dot-dashed line; $L = 100$ Å, dashed line; $L = 200$ Å, dotted line. The four curves starting at $T = 200$ K represent hole temperatures, the others represent electron temperatures. This figure is Fig. 1 from Marchetti and Pötz.[34]

In Fig. 9, the electron and hole temperatures are displayed as functions of time for different layer thickness L. The exchange of energy between electrons and holes plays an important role in the initial stage of the relaxation. The main portion of the photon excess energy is given to the photogenerated electrons. Initially, the kinetic energy of excited holes is below the threshold for optical phonon emission. However, the $e-h$ coupling rapidly transfers energy from electrons to holes and thus ensures significant participation of the holes in the cooling process. This energy loss channel is also important after the buildup of LO-phonon modes which couple to electrons slows the cooling of electrons. Reabsorption of phonons becomes important within less than a picosecond after the onset of the laser pulse and leads to a considerable reduction of the carrier cooling rate in the later stage of the relaxation.

One can see, from Fig. 9, that the carrier cooling rate is rather insensitive to variations in the well thickness, if the sheet density is kept constant. This result is in agreement with experiment.[35]. On the other hand, their calculation[34] indicates that for given layer thickness and times beyond 0.5 ps, cooling occurs at a slow rate at higher values of sheet density, because of a strong buildup of nonequilibrium optical phonons at higher sheet density.

3.3. Electron-hole Transport and Negative Mobility

The luminescence measurements of the photoexcited electron-hole (e-h) plasma in quasi-2D quantum wells and the relative theoretical study, which was discussed in Sec. 3.2, are important to derive information about relaxation of this system. On the other hand, transport measurements of a photoexcited electron-hole system under an applied electric field have also provided some interesting results.[36,37] Recently, Höpfel, Shah, Wolff, and Gossard[37] found that in a such system the minority electrons, which are injected by laser pumps on the p-modulation-doped quantum wells, can move in the direction of the external electric field. This negative absolute mobility of electrons occurs because of strong electron-hole drag. This subject was theoretically studied by Cui, Lei, and Horing[38] and by us[39].

We first briefly discuss the condition for negative absolute mobility of electrons in the region of weak electric field where the conductivity is linear. In the steady state we have the force balance equation for carriers:

$$n_\mu e_\mu \mathbf{E} - \mathbf{F}^{\mu-\nu} - \mathbf{F}^{\mu-L} = 0 , \tag{3.9}$$

where $\mathbf{E}$ is the external electric field, $\mathbf{F}^{\mu-L}$ represents the frictional force due to the carrier-lattice interaction and $\mathbf{F}^{\mu-\nu}$ represents the frictional force upon the μ-type carriers due to the carrier-carrier interaction with the ν-type carriers. It is obvious that $\mathbf{F}^{\mu-\nu} = -\mathbf{F}^{\nu-\mu}$. In the region of linear conductivity we have

$$\mathbf{F}^{\mu-L} = n_\mu A^{\mu-L} \mathbf{v}_\mu \ , \tag{3.10}$$

$$\mathbf{F}^{\mu-\nu} = n_\mu n_\nu A^{\mu-\nu} (\mathbf{v}_\mu - \mathbf{v}_\nu) \ , \tag{3.11}$$

where $\mathbf{v}_\mu$ is the drift velocity of μ type of carriers, $A^{\mu-L}$ represents the contribution to the resistivity (per carrier) from μ–L scattering, and $A^{\mu-\nu}$ relates to the contribution to the resistivity (per carrier μ) from μ–ν scattering normalized to per carrier ν. From Eqs. (3.9) - (3.11) we immediately obtain the mobility for electrons, μ_e:

$$\mu_e = \frac{(n_e - n_h) A^{e-h} + A^{h-L}}{A^{e-L} A^{h-L} + n_e A^{e-h} A^{e-L} + n_h A^{e-h} A^{h-L}} \ . \tag{3.12}$$

Equation (3.12) indicates that for electrons a negative absolute mobility is only possible when $n_e < n_h$. (The corresponding statment for hole mobility could require $n_h < n_e$.) It is determined by the difference between the density of electrons and the density of holes, and the competition between electron-hole drag and hole-lattice scattering. At low temperature and under a weak electric field, the former dominates, so the mobility of electrons is negative. When the lattice temperature or the electric field increase, the latter tends to dominate and the *mobility of minority electrons* becomes positive.

The carrier dynamics is derived in a similar way as discussed in Sec. 3.1 and Sec. 3.2. We separate the center-of-mass motion of each type of carrier from its relative motion. The 2D momentum for μ-type carriers in the relative coordinates is defined as $\hbar\bar{\mathbf{k}} = \hbar\mathbf{k} - m_\mu \mathbf{v}_\mu$ and a Fermi-Dirac distribution function is assumed at temperature T_μ, $\bar{f}^{\mu}_{\bar{\mathbf{k}}}(T_\mu)$, in the relative coordinates. The exchange of momentum and energy in the relative coordinates can then be written as

$$\bar{\mathbf{k}} - \bar{\mathbf{k}}' = \mathbf{q} \ , \qquad \bar{E}^{\mu}_{\bar{\mathbf{k}}} - \bar{E}^{\mu}_{\bar{\mathbf{k}}'} = \hbar(\omega - \mathbf{q}\cdot\mathbf{v}_\mu) \ . \tag{3.13}$$

A set of coupled equations for the time evolution of the drift velocities of the center-of-mass and energies in the relative coordinates for each type of carrier can be derived. We obtain

$$\frac{\partial n_\mu m_\mu \mathbf{v}_\mu(t)}{\partial t} = e_\mu n_\mu \mathbf{E} - \sum_L \mathbf{F}^{\mu-L}(t) - \mathbf{F}^{\mu-\nu}(t) \ , \tag{3.14}$$

and

$$\frac{\partial \bar{E}^{\mu}(t)}{\partial t} = -\sum_L \frac{\partial \bar{E}^{\mu-L}(t)}{\partial t} - \frac{\partial \bar{E}^{\mu-\nu}(t)}{\partial t} \ . \tag{3.15}$$

$\mathbf{F}^{\mu-L}$ in Eq. (3.14) represents the frictional force due to carrier-lattice (impurity) interaction. The expression of, for example, LO phonons is similar to Eqs. (3.3) - (3.6). Here, the carrier interactions with LO, TO, acoustic phonons, and impurities are considered. Also, the hot-

phonon effects for LO and TO phonons are included. $\mathbf{F}^{\mu-\nu}$, which represents the frictional force due to e-h scattering, with ν a different type of carrier than μ, is given by

$$\mathbf{F}^{\mu-\nu} = \frac{2\pi}{\hbar} \sum_{\mathbf{q}} \sum_{i,j} \sum_{i',j'} \sum_{\mathbf{k}',\mathbf{k}} \sum_{\mathbf{p}',\mathbf{p}} \hbar\mathbf{q}\, f^{\mu}_{i\mathbf{k}}(1-f^{\mu}_{i'\mathbf{k}'}) f^{\nu}_{j\mathbf{p}}(1-f^{\nu}_{j'\mathbf{p}'}) \mid \tilde{V}^{\mu\nu}_{ij,\,i'j'}(\mathbf{q},\,\omega) \mid^2 \delta_{\mathbf{k}',\mathbf{k}-\mathbf{q}} \delta_{\mathbf{p}',\mathbf{p}+\mathbf{q}}$$

$$\times \delta[E^{\mu}_{i\mathbf{k}} + E^{\nu}_{j\mathbf{p}} - E^{\mu}_{i'\mathbf{k}'} - E^{\nu}_{j'\mathbf{p}'} + \hbar\mathbf{q}\cdot(\mathbf{v}_{\mu}-\mathbf{v}_{\nu})] \,. \tag{3.16}$$

where the term $\hbar\mathbf{q}\cdot(\mathbf{v}_{\mu}-\mathbf{v}_{\nu})$ appears in the last δ function because the energies E for electrons and holes are defined in different coordinates, and $\omega = (E^{\mu}_{i\mathbf{k}} - E^{\mu}_{i'\mathbf{k}'})/\hbar$. The last term in Eq. (3.15) represents the energy loss rate in the relative system due to e-h scattering. An equation for the rate of energy loss can be obtained by replacing $\mathbf{F}^{\mu-\nu}$ in Eq. (3.16) by $-dE^{\mu-\nu}(t)/dt$ and the prefactor $\hbar\mathbf{q}$ on the right hand side of Eq. (3.16) by $E^{\mu}_{i\mathbf{k}} - E^{\mu}_{i'\mathbf{k}'}$.

The term $\tilde{V}^{\mu\nu}_{ij,\,i'j'}(\mathbf{q},\,\bar{\omega})$ in Eq. (3.16) represents the 2D screened scattering matrix between carriers. Here, one should be careful in treatment of screening effect when two kinds of carriers coexist. The unscreened electron-electron, hole-hole, and electron-hole scatterings occur via Coulomb interactions given by

$$[V^{\mu\nu}(q)]_{ij,\,i'j'} = \frac{2\pi e_{\mu} e_{\nu}}{\varepsilon_0 q A} F^{\mu\nu}_{ij,\,i'j'}(q) \,, \tag{3.17}$$

where the form factor $F^{\mu\nu}_{ij,\,i'j'}(q)$ is given by Eq. (2.26), and ε_0 is the static dielectric constant. Since the strength of the electron-hole interaction is of the same order as the electron-electron interaction and the hole-hole interactions, the dynamic screening effect should be expressed by a more complex form than that in the case of a single type of carrier. These interactions are shown in Fig. 10 in the random phase approximation (RPA). According to Fig. 10, the screened carrier-carrier scattering matrix, $\tilde{V}^{\mu\nu}$, satisfies the following equation:

$$\tilde{V}^{\mu\nu} = V^{\mu\nu} + \sum_{\eta} V^{\mu\eta} \Pi^{\eta} \tilde{V}^{\eta\nu} \,. \tag{3.18}$$

where Π^{η} is a diagonal matrix, its elements are the density-density correlation functions for 2D carriers. If we define

$$\tilde{V} = \begin{bmatrix} \tilde{V}^{ee} & \tilde{V}^{eh} \\ \tilde{V}^{he} & \tilde{V}^{hh} \end{bmatrix}, \qquad \Pi = \begin{bmatrix} \Pi^{e} & 0 \\ 0 & \Pi^{h} \end{bmatrix}, \qquad V = \begin{bmatrix} V^{ee} & V^{eh} \\ V^{he} & V^{hh} \end{bmatrix}, \tag{3.19}$$

The screened carrier-carrier scattering matrix can then be expressed in matrix form:

$$\tilde{V} = [\,1 - V\cdot\Pi\,]^{-1} V \tag{3.20}$$

When only the lowest band for electrons and holes are occupied, $\tilde{V}$ can be straightforwardly written as

$$\tilde{V} = \frac{1}{\Lambda}\begin{bmatrix} (1-V^{hh}\Pi^h)V^{ee}+V^{eh}\Pi^h V^{he} & V^{eh} \\ V^{he} & (1-V^{ee}\Pi^e)V^{hh}+V^{he}\Pi^e V^{eh} \end{bmatrix}, \tag{3.21}$$

with

$$\Lambda = (1-V^{ee}\Pi^e)(1-V^{hh}\Pi^h) - V^{eh}\Pi^h V^{he}\Pi^e . \tag{3.22}$$

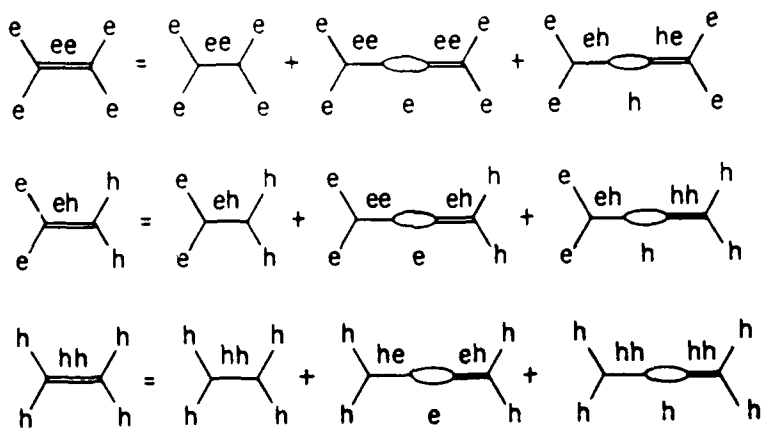

Fig. 10. Diagrams for screening effect of carrier-carrier potential in the RPA. The single and double horizontal solid lines represent, respectively, the unscreened and screened carrier-carrier interaction, $V^{\mu\nu}$ and $\tilde{V}^{\mu\nu}$. The bubble represents the density-density correlation function, Π^{μ}.

Solving a set of coupled equations, Eqs. (3.14) and (3.15) and corresponding equations for hot-phonons, we can determine the $\mathbf{v}_e$, $\mathbf{v}_h$, T_e, T_h as well as the distribution of hot-phonon wavepackets (LO, TO). The mobilities for both carriers in a weak electric field are shown in Fig. 11 as functions of lattice temperature, T_L. Fig. 12 shows the weak field mobility of electrons and holes as functions of the electron density, n_e.

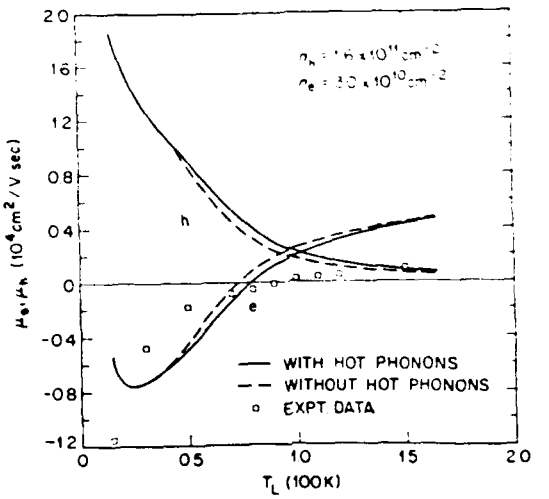

Fig. 11. Mobility of electrons, μ_e, and mobility of holes, μ_h, as functions of lattice temperature, T_l, in a weak electric field. Data for electron mobility come from Höpfel *et al*[3].

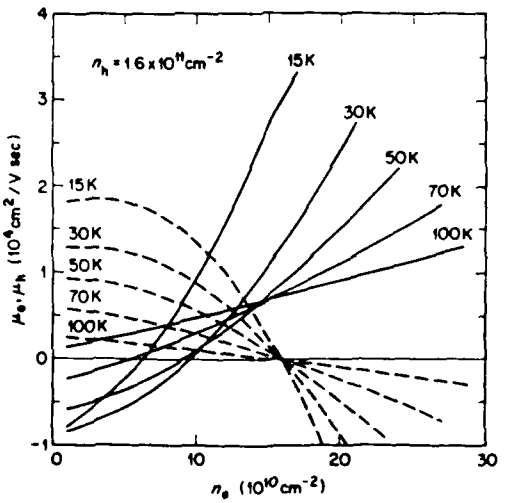

Fig. 12. Mobility of electrons, μ_e (solid curves), and mobility of holes, μ_h (dashed curves), as functions of density of electrons, n_e, at different lattice temperature, T_l (in a weak electric field).

4. OTHER THEORETICAL WORKS

4.1. Monte Carlo Simulation of Nonequilibrium Phonon effect

In the above discussion a simplifying assumption for the carrier distribution function, namely, that is a Fermi-Dirac function at the carrier temperature T, is assumed. This assumption usually is a good one for the high carrier density and for the time scale larger than pecosecond. However, recent progress in ultrafast experiments leads to processes in which the carrier distribution can not be regard as in quasi-equilibrium. Use of Monte Carlo techniques to solve the dynamical equation on the supercomputer is the way of obtaining the nonequilibrium carrier distribution. Lugli *et al* have presented a series theoretical results on nonequilibrium phonon effects based on a novel Monte Carlo algorithm.[20,40–42] They have calculated the results for both the bulk and quantum well cases. In the case of a quantum well, the effect of several subbands has been included. However, a simple model was used, that is, that the q_z, components of the phonon distribution are localized in a region of wavevector space of extent $1/L$, with L the width of well.

The physics of the dynamical evolution of the carrier-phonon system is very similar to what we have discussed. The coupled Boltzmann equations are given by

$$\frac{\partial f_{\mathbf{k}}}{\partial t} = \left[\frac{\partial f_{\mathbf{k}}^{(i)}}{\partial t}\right]_{e-\text{ph}} + \left[\frac{\partial f_{\mathbf{k}}^{(i)}}{\partial t}\right]_{e-e} + \left[\frac{\partial f_{\mathbf{k}}^{(i)}}{\partial t}\right]_{e-\text{imp}}, \tag{4.1}$$

$$\frac{\partial N_{\mathbf{q}}^{(j)}}{\partial t} = \left[\frac{\partial N_{\mathbf{q}}^{(j)}}{\partial t}\right]_{\text{ph}-e} + \left[\frac{\partial N_{\mathbf{q}}^{(j)}}{\partial t}\right]_{\text{ph}-\text{ph}}, \tag{4.2}$$

where the superscripts i and j indicate, respectively, the type of carrier (electron or holes) and of phonon modes (LO, TO, . . .) considered. $(\partial N_{\mathbf{q}})/\partial t \mid_{\text{ph}-\text{ph}}$ is obtained by relaxation time approximation, given by Eq. (2.24). Fig. 13 shows the evolution of the electron total energy as a function of time in an n-type quantum well during and after the laser pulse. The excited electrons lose energy mainly through the interaction with the background electrons and through the emission of LO phonons. A much slower relaxation is found when nonequilibrium phonon effects are included. Fig. 14 shows the LO-phonon distribution at different times.

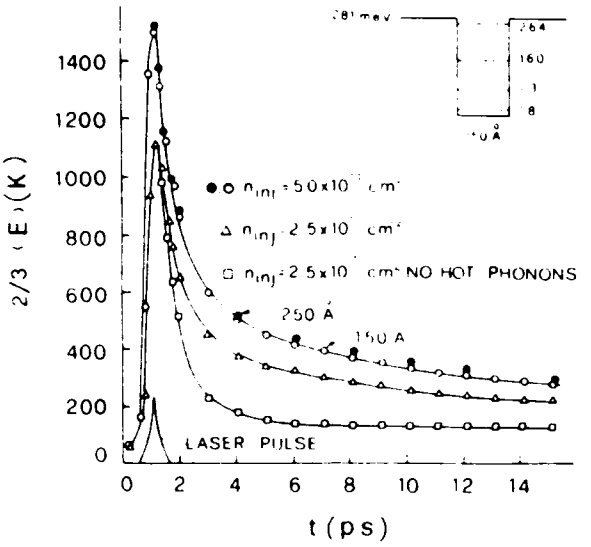

Fig. 13. Average electron energy, measured in equivalent temperature, as a function of time during and after the laser excitation for two different excitation sheet densities. The position of the energy levels in the well is shown in the insert. This figure is Fig. 12 from Lugli *et al.*[42]

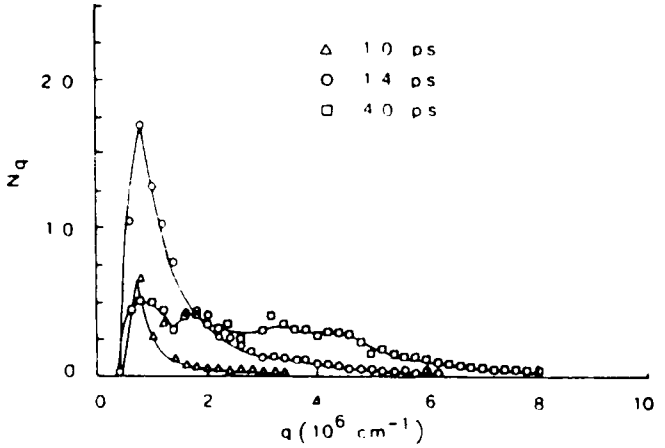

Fig. 14. LO-phonon distribution as a function of total parallel momentum (for $q_z = 0$) for times during and after the laser excitation. This figure is Fig. 13 from Lugli *et al.*[42]

When the laser photon energy is about 2 eV, photon-excitation in bulk GaAs includes transition from three hole bands. The energy distribution of photo-excited electrons is characterized by three distinct peaks, as shown in the insert of Fig. 15. In GaAs, about 60% of the photoexcited carriers transfer to the satellite valleys during the laser pulse (the average time for $\Gamma - L$ transition via phonon emission or absorption is about 80 fs). Carriers return slowly to the Γ valley, with characteristic time of 2 or 3 ps, because of smaller effective mass in the Γ valley. This leads a slow rise of luminescence in GaAs, as shown in Fig. 15.[42] In Fig. 15, a comparison to the InP case is also provided, where the L valley are located at a much high energy, and do not significantly contribute to the cooling process. By fitting data with the Monte Carlo calculation, it is determined that the Γ–L deformation potential $D_{\Gamma L}$ is $(6.5 \pm 1.5) \times 10^8$ eV/cm. This Γ–L exchange depletes the Γ electron distribution in GaAs in the high-energy region, above 0.3 eV, as shown in Fig. 16.

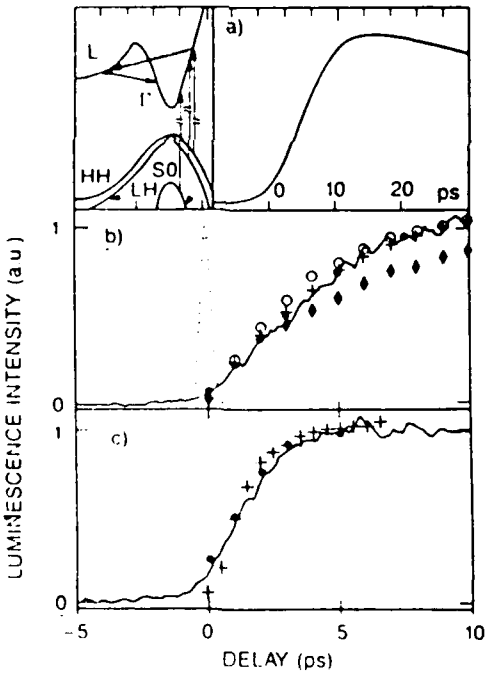

Fig. 15. Luminescence intensity at 300 K vs delay. (a) GaAs at 1.45 eV; (experiments) (b) the solid curve is the same as (a) on expanded scale; the filled circles show the spectrally integrated intensity; (c) InP, same as (b); Results of ensemble Monte Carlo calculations are also shown: (b) $D_{\Gamma L} = (4, 6, \text{and } 8) \times 10^8$ eV/cm for GaAs (lozenges, crosses, and open circles, respectively) and (c) InP. This figure is Fig. 2 from Shah *et al.*[41]

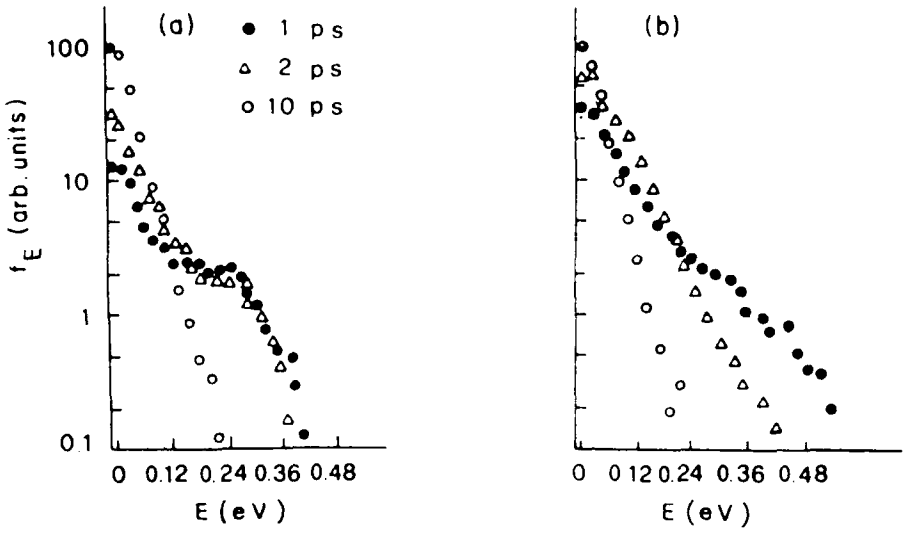

Fig. 16. The Monte Carlo results of the Energy distribution function for Γ-valley electrons in (a) GaAs and (b) InP at three different time delays after the excitation. The excitation density is 5×10^{16} cm^{-3} and the lattice temperature is 300 K. This figure is Fig. 16 from Lugli *et al.*[42]

4.2. Effect of LO-phonon renormalization

A series of works by Das Sarma and his coworkers[43–46] studied the hot-electron relaxation by emission of LO phonons in both 2D and 3D cases. In addition to the hot-phonon effect and dynamical screening, they found that many-body renormalization of the LO phonons also plays a crucial role in the power-loss process at low electron temperatures. Due to phonon-plasmon coupling, the density states of an LO phonon has three branches: (1) the bare-phonon-like branch near the bare-phonon energy, (2) the plasmonlike branch near the plasmon energy, and (3) the low-energy quasiparticle-excitation-like branch in the quasiparticle-excitation region. Even though the oscillator strength of plasmonlike and the quasiparticle-excitation-like branchs are extremely small, they dominate the power-loss process at low enough electron temperatures that most electrons have energy below the threshold for bare LO phonon emission. This produces an enhancement of the power loss at low electron temperatures by many orders of magnitude relative to the power loss to bare LO phonons.

The phonon density of states, $A(q, \omega)$ is given by

$$A(q, \omega) = -\pi^{-1} \operatorname{Im} D(q, \omega) \tag{4.3}$$

where D is the phonon propagator. For bare phonons, D is replaced by $D^{(0)}$.

$$D^0(q,\omega) = \frac{2\omega_L}{\omega^2 - \omega_L^2}, \tag{4.4}$$

and $\mathrm{Im}\,D^0(q,\omega) = -\pi|\delta(\omega-\omega_L)-\delta(\omega+\omega_L)|$, which has vanishing weight everywhere except at the bare energy. By introducing the phonon-plasmon coupling in the random phase approximation (RPA), the renormalized phonon propagator is obtained by

$$D(q,\omega) = \frac{2\omega_L}{\omega^2 - \omega_L^2 - 2\omega_L M_q^2 \Pi(q,\omega)}, \tag{4.5}$$

where M_q is the electron-phonon matrix element, and $\Pi(q,\omega)$ is the electron density-density correlation function. Fig. 17 displays the renormalized phonon spectral function for the 3D and 2D cases. Three branches of phonon modes are shown. Note that the scale factor γ in Fig. 17 is different for different curves. The strength of the plasmonlike phonon is very small, the quasiparticle-excitation-like (QPE-like) mode is also weak. However, it is found that the QPE-like phonons dominate the hot-electron power-loss process at low electron temperatures.

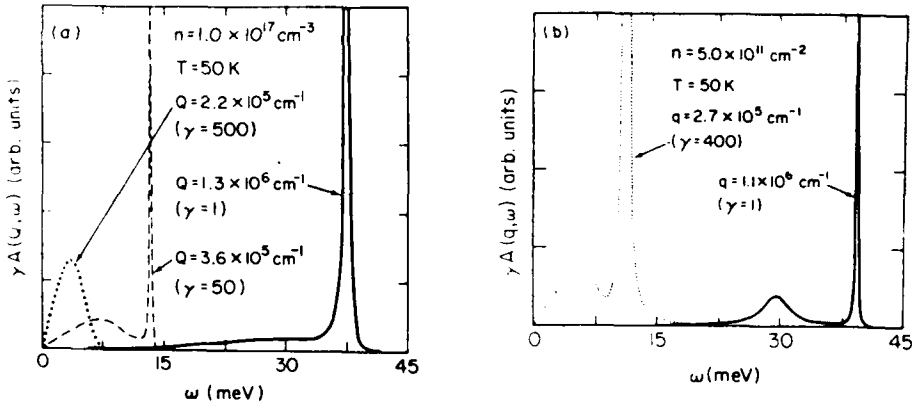

Fig. 17. (a) Phonon spectral function for three wave vectors in a 3D electron gas at an electron temperature of $T = 50\,\mathrm{K}$ ($T_L = 0$). For $Q = 2.2\times10^5\ \mathrm{cm}^{-1}$, the QPE branch extends from 0 to 7 meV, and there are δ-function peaks near the plasmon energy ($\omega_p = 14$ meV) and the phonon energy (36.8 meV), which are not shown explicitly in order to avoid too much detail. For $Q = 3.6\times10^5\ \mathrm{cm}^{-1}$ the QPE branch extends to ~14 meV, and there is again a δ-function peak (not shown) at ω_L. For $Q = 1.3\times10^6\ \mathrm{cm}^{-1}$ the plasmonlike phonon is Landau damped, and the QPE-like phonons extend all way up to ω_L. The electron density is $10^{17}\ \mathrm{cm}^{-3}$, giving a Fermi vector of $1.4\times10^6\ \mathrm{cm}^{-1}$. (b) Phonon spectral function for two different wave vector in a 2D electron gas. For $q = 2.7\times10^5\ \mathrm{cm}^{-1}$ there is a δ-function peak (not shown) at ω_L. The electron density is $5\times10^{11}\ \mathrm{cm}^{-2}$ giving a Fermi vector of $1.8\times10^6\ \mathrm{cm}^{-1}$. This Figure is Fig.4 from Das Sarma.[16]

At low temperature (about 50 K) the number of electrons which can emit phonon with bare-mode phonons becomes extremely small. However, phonon-plasmon coupling creates new low-energy modes, even though its strength is rather small, they could make important contribution in energy loss at low electron temperature. In this case, Eq. (2.32) for the energy loss rate is no longer valid since it was derived by considering only bare LO phonon modes. Instead, Das Sarma *at al* derived the following expression for power loss by generalizing the Kogan formula[47] to including phonon self-energy correction:

$$P=\sum_q \int \frac{d\omega}{\pi}\omega M_q^2 |n_{T_L(\omega)}-n_T(\omega)|\,\mathrm{Im}\Pi(q,\omega)\mathrm{Im}D(q,\omega)\,, \tag{4.6}$$

where $n_T=|\exp(\omega/k_BT)-1|^{-1}$.

In order to include the hot-phonon effect, one must first rewrite Eq. (4.6) as

$$P=\sum_q \int d\omega\,\omega R(q,\omega)n_T(\omega)\,, \tag{4.7}$$

then replace $R(q,\omega)$ in the integrand by $R(q,\omega)/[1+\tau_{op}R(q,\omega)]$. Das Sarma *et al* suggest that only the bare phonon mode is important for hot-phonon effects.

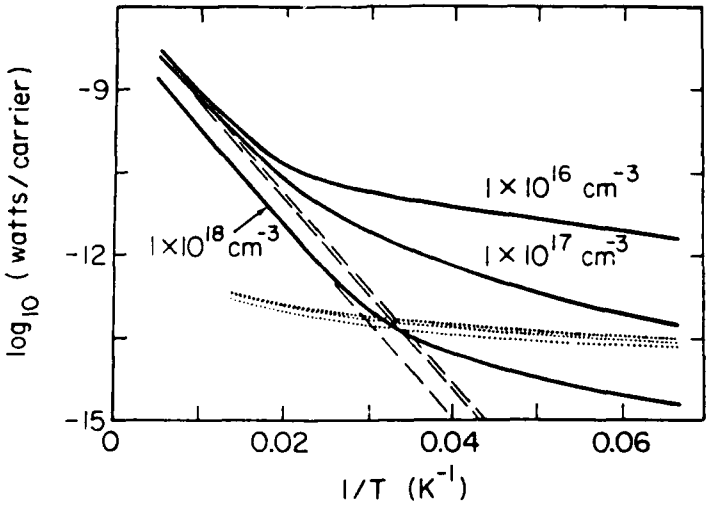

Fig. 18. Power loss as a function of the inverse electron temperature for 3D electron gas (solid lines), the dashed lines correspond to power loss to bare LO phonons only. The doted lines give the power loss to acoustic-phonon modes. For dotted curves, the uppermost curve is for 10^{18} cm^{-3}, the middle one for 10^{16} cm^{-3}, and the lowest one for 10^{17} cm^{-3}. $T_L=0$, and the power loss is expressed in watts per carrier. This figure is Fig. 5 from Das Sarma *et al.*[46]

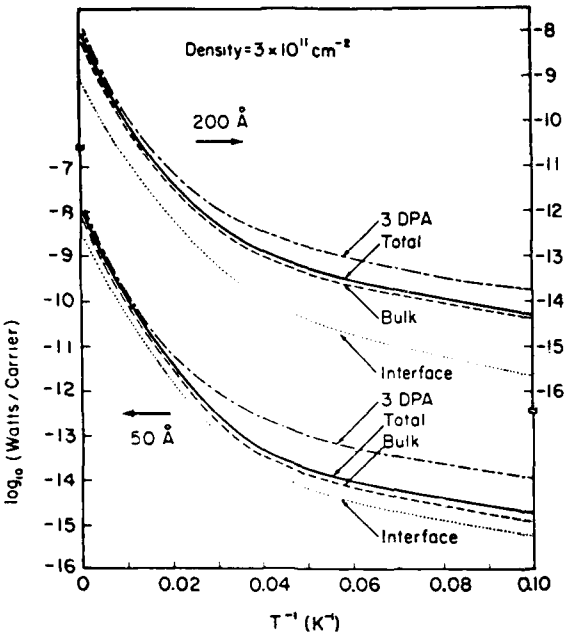

Fig. 19. Power loss as function of inverse electron temperature for two quantum wells (width 50 and 200Å) calculated in 3D phonon approximation (3DPA) and in slab-model. $T_L = 0$, and the power loss is expressed in watts per carrier. This figure is Fig. 1 from Das Sarma *et al.*[45]

At high temperatures ($T \geq 50$ K) the bare LO phonons dominate the power loss, at intermediate temperatures ($20 < T \leq 50$ K) power is lost predominantly to the plasmonlike or QPE-like branch of the LO-phonon spectrum, and at still lower temperatures ($T \leq 20$ K) the acoustic phonons become important. Fig. 18 shows the power loss for 3D electron gas at lattice temperature $T_L = 0$. Fig. 19 shows the results in quantum wells.

Recently, M. W. C. Dharma-wardana[48] deals with the same subject using nonequilibrium Green's function approach. He considers not only the coupled-mode spectral density, but also the coupled-distribution functions. In contrast to Das Sarma and co-workers, he found that the energy-loss rate is significantly suppressed by coupled-mode formation and quasiparticlelike modes do not contribute to the energy-loss rate. The underlying physical picture is that although the coupled-mode phonon spectral density has some weight in the quasiparticlelike region of energies, these coupled-phonon modes are effectively at electron temperature, not at lattice temperature. Hence there is no enhancement. Nevertheless, coupled-mode phonons are hotter than bare phonons and this leads to a suppression of energy-lose rate.

5. SUMMARY

We have reviewed in this paper the effect of reabsorption of nonequilibrium optical phonons on the carrier relaxation and transport. Both experiments and theoretical study confirm that the build-up of hot-phonons is mainly responsible for reducing the cooling rate of photo-excited electrons, while the dimensionality and dynamical screening effect play only a minor role. In the case of heterojunctions or quantum wells, our approach can determine the accurate shape of the phonon wave packet and produce a simple procedure for calculating the effect of nonequilibrium phonons. Our results are in quantitative agreement with experiments. On the other hand, the cooling of photo-excited carriers is a rich field, which may involve the electron-hole (three kind of holes) interaction, multi-valleys and multi-subband transitions, multi-scattering processes, from very high temperature down to very low-temperature. As examples, we refer to the effects of Γ–L transitions, which delay the build-up of hot Γ electrons in a ultrafast process, and what is the role of phonon-plasmon modes. There are many other factors, which may affect the relaxation process, such as phonon modes (interface and slab modes in quantum wells)[45] and LO phonon relaxation mechanism.[41] This subject is worthy of further study.

ACKNOWLEDGMENT

The work in the City College of City University of New York was partly supported by the U. S. Army Research Office and the U. S. Department of Energy.

Appendix

In this appendix the complete expressions for Eqs. (2.13) and (2.14) are given as follows:

$$\left[\frac{\partial f_{n\mathbf{k}}}{\partial t}\right]_{ep} = \frac{2\alpha^2}{\hbar A} 2\pi \sum_{\mathbf{q}} \sum_{q_z} \sum_{q_z'} \sum_{n'\mathbf{k}'} G^*_{nn'}(\mathbf{q}, q_z) G_{nn'}(\mathbf{q}, q_z')$$

$$(\{ f_{n'\mathbf{k}'}(t)[1 - f_{n\mathbf{k}}(t)]\delta_{\mathbf{k}',\mathbf{k}+\mathbf{q}}\delta(E_{n'\mathbf{k}'} - E_{n\mathbf{k}} - \hbar\omega_L)$$

$$- f_{n\mathbf{k}}(t)[1 - f_{n'\mathbf{k}'}(t)]\delta_{\mathbf{k}',\mathbf{k}-\mathbf{q}}\delta(E_{n\mathbf{k}} - E_{n'\mathbf{k}'} - \hbar\omega_L)\}[\delta_{q_z q_z'} + n_{\mathbf{q}}(q_z, q_z', t)]$$

$$+ \{ f_{n'\mathbf{k}'}(t)[1 - f_{n\mathbf{k}}(t)]\delta_{\mathbf{k}',\mathbf{k}-\mathbf{q}}\delta(E_{n'\mathbf{k}'} - E_{n\mathbf{k}} + \hbar\omega_L)$$

$$-f_{n\mathbf{k}}(t)[1-f_{n'\mathbf{k}'}(t)]\delta_{\mathbf{k}',\mathbf{k}+\mathbf{q}}\delta(E_{n\mathbf{k}}-E_{n'\mathbf{k}'}+\hbar\omega_L)\}n_{\mathbf{q}}(q_z, q_z', t)) \tag{A.1}$$

$$\left[\frac{\partial n_{\mathbf{q}}(q_z, q_z', t)}{\partial t}\right]_{ep} = \frac{2\alpha^2}{\hbar A}\lim_{\varepsilon\to 0^+}\sum_{n\mathbf{k}}\sum_{n'\mathbf{k}'}\sum_{q_z''} f_{n\mathbf{k}}(t)\,[1-f_{n'\mathbf{k}'}(t)]$$

$$\cdot\left[\delta_{\mathbf{k}',\,\mathbf{k}-\mathbf{q}}\,\frac{G_{n'n}(\mathbf{q}, q_z)\,G^*_{n'n}(\mathbf{q}, q_z'')}{\varepsilon - i[E_{n\mathbf{k}}-E_{n'\mathbf{k}'}-\hbar\omega_L]}[\delta_{q_z'', q_z'}+n_{\mathbf{q}}(q_z'', q_z', t)]\right.$$

$$+\delta_{\mathbf{k}',\,\mathbf{k}-\mathbf{q}}\,\frac{G^*_{n'n}(\mathbf{q}, q_z')\,G_{n'n}(\mathbf{q}, q_z'')}{\varepsilon + i[E_{n\mathbf{k}}-E_{n'\mathbf{k}'}-\hbar\omega_L]}[\delta_{q_z'', q_z}+n_{\mathbf{q}}(q_z, q_z'', t)]$$

$$-\delta_{\mathbf{k}',\,\mathbf{k}+\mathbf{q}}\,\frac{G_{n'n}(\mathbf{q}, q_z)\,G^*_{n'n}(\mathbf{q}, q_z'')}{\varepsilon + i[E_{n\mathbf{k}}-E_{n'\mathbf{k}'}+\hbar\omega_L]}n_{\mathbf{q}}(q_z'', q_z', t)]$$

$$\left.-\delta_{\mathbf{k}',\,\mathbf{k}+\mathbf{q}}\,\frac{G^*_{n'n}(\mathbf{q}, q_z')\,G_{n'n}(\mathbf{q}, q_z'')}{\varepsilon - i[E_{n\mathbf{k}}-E_{n'\mathbf{k}'}+\hbar\omega_L]}n_{\mathbf{q}}(q_z, q_z'', t)\right]. \tag{A.2}$$

[1]T. Ando, A. B. Fowler, and F. Stern, Rev. Mod. Phys. 54, 437 (1982)

[2]J. Shah, A. Pinczuk, A. C. Gossard, and W. Wiegmann, Phys. Rev. Lett. 54, 2045 (1985)

[3]J. Shah, A. Pinczuk, H. L. Störmer, A. C. Gossard, and W. Wiegmann, Appl. Phys. Lett. 44, 322 (1984)

[4]J. F. Ryan, R. A. Taylor, A. J. Turberfield, A. Maciel, J. M. Worlock, A. C. Gossard and W. Wiegmann, Phys. Rev. Lett. 53, 1841, (1984).

[5]D. K. Ferry, Surf. Sci. 75, 86 (1978)

[6]K. Hess, Appl. Phys. Lett. 35, 484 (1979)

[7]B. K. Ridley, J. Phys. C 15, 5899 (1982); 16, 6971 (1983)

[8]C. H. Yang, J. M. Carlson-Swindle, S. A. Lyon, and J. A. Worlock, Phys. Rev. Lett 55, 2359 (1985).

[9]W. W. Rühle and H. J. Polland, Phys. Rev. B 36, 1683 (1987).

[10]P. Price, Ann. Phys. (NY) 313, 217, (1981), Surf. Sci. 31B, 199, (1985)

[11]W. Pötz and P. Kocevar, Phys. Rev. B 28, 7040 (1983).

[12]W. Cai, M. C. Marchetti, and M. Lax, Phys. Rev. B 334, 8573 (1986, Dec. 15)

[13]W. Cai, M. C. Marchetti, and M. Lax, Phys. Rev. B 35, 1369 (1987, Jan. 15)

[14]R. Zwanzig, J. Chem. Phys. 33, 1338 (1960)

[15]R. Zwanzig, Phys. Rev. 124, 983 (1961)

[16]D. N. Zubarev, Nonequilibrium Statistical Thermodynamics (Consultant's Bureau, NY, 1974)

[17]S. Peletminskii and A. Yatsenko, Zh. Eksp. Teor. Fiz. 53, 1327 (1967) Sov. Phys. JETP 26, 773 (1968)

[18]See for instance: M. Born and K. Huang, *Dynamical Theory of Crystal Lattices* (Oxford University, Oxford, 1985), pp. 82-100.

[19]D. Von der Linde, J. Kuhl, and H. Klingenberg, Phys. Rev. Lett. 44, 1505 (1980).

[20]P. Lugli and S. M. Goodnick, Phys. Rev. Lett. 59, 716 (1987)

[21]M. A. Osman and D. K. Ferry, Phys. Rev. B 36, 6018 (1987)

[22]D. W. Bailey, M. A. Artaki, C. J. Stanton, and K. Hess, Appl. Phys. Lett. 62, 4638 (1987)

[23]S. M. Goodnick and P. Lugli, Phys. Rev. B 38, 10135 (1988)

[24]T. F. Zheng, W. Cai, P. Hu, and M. Lax, Phys. Rev. B 40, 1271 (1989)

[25]M. Lax, W. Cai, and M. C. Marchetti, "Nonequilibrium Phonon Dynamics in a Semiconductor Quantum Well", Proceeding of ultrafast laser probe phenomena in bulk and microstructure semiconductors II SPIE symposium, 208, (1988).

[26]M. C. Marchetti and W. Cai, Phys. Rev. B 35, 7725 (1987).

[27]J. Shah, A. Pinczuk, A. C. Gossard, W. Weigmann, and K. Kash, Surf. Sci. 174, 363 (1986)

[28]X. L. Lei and N. J. M. Horing, Phys. Rev B 35, 6281 (1987).

[29]W. Cai, M. C. Marchetti and M. Lax, Phys. Rev. B 37, 2636 (1988).

[30]J. R. Barker, J. Physics C 6, 1663 (1973)

[31]S.K. Sarker, Phys. Rev. B 33, 7263 (1986)

[32]M. Keever, W. Kopp, T. J. Drummond, H. Morko, and K. Hess, Jpn. J. Appl. Phys. 21, 1489 (1982)

[33]W. Pötz, Phys. Rev. B 36, 5016 (1987).

[34]M. C. Marchetti and Pötz, J. Vac. Sci. Techonol. B 6, 1341 (1988); Phys. Rev. B 40, 12391 (1989).

[35]K. Leo, W. W. Rühle, H. J. Queisser, and K. Ploog, Phys. Rev. B 37, 7121 (1988).

[36]R. A. Höpfel, J. Shah, and A. C. Gossard, Phys. Rev. Lett. 56, 765 (1986).

[37]R. A. Höpfel, J. Shah, P. A. Wolff, and A. C. Gossard, Phys. Rev. Lett. 56, 2736 (1986).

[38]H. L. Cui, X. L. Lei, and N. J. M. Horing, Phys. Rev. B 37, 8223 (1988).

[39]W. Cai, T. F. Zheng, and M. Lax, Phys. Rev. B 37, 8205 (1988).

[40]P. Lugli, C. Jacoboni, L. Reggiani, and P. Kocevar, Appl. Phys. Lett. 50, 1251 (1987)

[41]J. Shah, B. Deveaud, J. C. Damen, W. T. Tsang, A. C. Gossard, and P. Lugli, Phys. Rev. Lett. 59, 2222 (1987).

[42]P. Lugli, P. Bordone, L. Reggiani, M. Rieger, P. Kocevar, and S. M. Goodnick, Phys. Rev. B 39, 7852 (1989).

[43]Das Sarma, J. K. Jain, and R. Jalabert, Phys. Rev. B 37, 1228 (1988); 37, 4560 (1988); 37, 6290 (1988).

[44]K. Jain, R. Jalabert, and S. Das Sarma, phys. Rev. Lett. 60, 353 (1988); 61, 2005(E) (1988).

[45]K. Jain and S. Das Sarma, Phys. Rev. Lett. 62, 2305 (1989).

[46]Das Sarma, J. K. Jain, and R. Jalabert, Phys. Rev. B 41, 3561 (1990).

[47]Sh. M. Kogan, Sov. Phys.--Solid State 4, 1813 (1963).

[48]M. W. C. Dharma-wardana, Phys. Rev. Lett. 66, 197 (1991).